

**The Iron Chelator, Deferasirox, as a Novel Strategy for Cancer Treatment:
Oral Activity Against Human Lung Tumor Xenografts and Molecular
Mechanism of Action.**

**Goldie Y.L. Lui, Peyman Obeidy, Samuel J. Ford, Chris Tselepis, Danae M. Sharp, Patric
J. Jansson, Danuta S. Kalinowski, Zaklina Kovacevic, David B. Lovejoy and Des R.
Richardson**

*Iron Metabolism and Chelation Program, Department of Pathology and Bosch Institute,
University of Sydney, Sydney, New South Wales, 2006, Australia (G.Y.L.L., P.O., D.M.S., P.J.J.,
D.S.K., Z.K., D.B.L. and D.R.R.) and School of Cancer Sciences, University of Birmingham,
Vincent Drive, Birmingham B15 2TT, United Kingdom (S.J.F. and C.T.).*

Running Title: Deferasirox as a New Strategy for the Treatment of Cancer

Author for Correspondence: Dr. D. R. Richardson, Iron Metabolism and Chelation Program, Department of Pathology and Bosch Institute, University of Sydney, Sydney, New South Wales, 2006 Australia. Ph: +61-2-9036-6548; +61-2-9036-6549; Email: d.richardson@med.usyd.edu.au.

Number of Pages: 41

Number of Tables: 3 plus 1 Supplementary Table

Number of Figures: 7 plus 1 Supplementary Figure

Number of References: 60

Word Count:

- Abstract: 242
- Introduction: 722
- Discussion: 1497

Abbreviations:

3-AP, 3-aminopyridine-2-carboxaldehyde thiosemicarbazone; BpT, 2-benzoylpyridine thiosemicarbazone; DFO, desferrioxamine; DpT, di-2-pyridylketone thiosemicarbazone; Dp44mT, di-2-pyridylketone 4,4-dimethyl-3-thiosemicarbazone; MTD, maximum tolerated dose; MTT, 3-(4,5-dimethylthiazol)-2,5-diphenyl tetrabromide; NDRG1, N-myc down-stream regulated gene 1; PARP1, poly (ADP-ribose) polymerase 1; ROS, reactive oxygen species; RR, ribonucleotide reductase; Tf, human transferrin; TfR1, transferrin receptor-1.

Abstract

Deferasirox is an orally-effective iron chelator currently used for the treatment of iron (Fe) overload disease and has been implemented as an alternative to the “gold standard” chelator, desferrioxamine (DFO). Earlier studies demonstrated that DFO has anti-cancer activity due to its ability to deplete cancer cells of Fe. In this investigation, we examined the *in vitro* and *in vivo* activity of deferasirox against cells from human solid tumors. To date, there have been no studies to investigate the effect of deferasirox on these types of tumors *in vivo*. Deferasirox demonstrated similar activity at inhibiting proliferation of DMS-53 lung carcinoma and SK-N-MC neuroepithelioma cell lines when compared to DFO. Further, deferasirox was generally similar or slightly more effective than DFO at mobilizing cellular ^{59}Fe and inhibiting iron uptake from Tf depending on the cell-type. However, deferasirox potently inhibited DMS-53 xenograft growth in nude mice when given by oral gavage, with no marked alterations in normal tissue histology. To understand the anti-tumor activity of deferasirox, we investigated its effect on the expression of molecules that play key roles in metastasis, cell cycle control and apoptosis. We demonstrated that deferasirox increased expression of the metastasis suppressor protein, N-myc downstream regulated gene-1 (NDRG1), and up-regulated the cyclin-dependent kinase inhibitor p21^{CIP1/WAF1}, while decreasing cyclin D1 levels. Moreover, this agent increased the expression of apoptosis markers, including cleaved caspase-3 and cleaved poly [ADP-ribose] polymerase 1. Collectively, we demonstrate that deferasirox is an orally-effective anti-tumor agent against solid tumors.

Introduction

Cells require iron (Fe) for numerous important cellular processes including energy generation, oxygen transport and DNA synthesis (Kalinowski and Richardson, 2005; Whitnall et al., 2006). Iron is able to cycle between two stable redox states, the ferric [Fe(III)] and ferrous [Fe(II)] forms, allowing it to act as an electron donor/acceptor (Kalinowski and Richardson, 2005). Consequently, iron can participate in the generation of cytotoxic reactive oxygen species (ROS) (Kalinowski and Richardson, 2005). Due to the deleterious effects of ROS, intracellular iron levels must be tightly regulated (Chua et al., 2007).

Iron chelators for clinical use were initially developed for the treatment of iron overload (Cappellini, 2007; Porter, 2009). Examples of clinically used iron chelators include deferiprone (Ferriprox[®]), deferasirox (Exjade[®]; Figure 1A) and the current “gold-standard” chelator, desferrioxamine (DFO; Figure 1B) (Kalinowski and Richardson, 2005). Since deferasirox is orally-active and has a longer plasma half-life than DFO, it is considered to be a better alternative as it avoids the long hours of subcutaneous administration that results in poor patient compliance with DFO (Hershko et al., 2001). Deferasirox at high doses can mobilize liver iron and has been shown to be effective and safe in clinical studies (Finkenstedt et al., 2010; Nick et al., 2009).

In recent years, the potential for iron chelators in the treatment of cancer has emerged. This reflects the fact that cancer cells typically require more iron than normal cells to mediate their generally rapid DNA synthesis and growth (Whitnall et al., 2006). Hence, depriving cancer cells of iron is a novel approach for cancer treatment (Kalinowski and Richardson, 2005). An iron chelator that has been specially developed for cancer therapy is 3-aminopyridine-2-

carboxaldehyde thiosemicarbazone (3-AP, or Triapine[®]; Figure 1C), which is currently in phase II clinical trials (Knox et al., 2007). However, this agent demonstrates low efficacy and serious side effects such as methemoglobinemia and hypoxia (Chaston et al., 2003; Kalinowski and Richardson, 2005; Yen et al., 2004). More recently, our laboratory has developed novel thiosemicarbazones, namely the dipyridyl thiosemicarbazone (DpT) and 2-benzoylpyridine thiosemicarbazone (BpT) series of iron chelators which have shown marked anti-proliferative activity both *in vitro* and *in vivo* (Kovacevic et al., 2011a; Yu et al., 2011a). One of the most effective compounds, di-2-pyridylketone-4,4,-dimethyl-3-thiosemicarbazone (Dp44mT; Figure 1D), has been shown to be more effective than 3-AP at inhibiting the growth of human tumor xenografts *in vivo* (Whitnall et al., 2006).

The reported mechanism of action of DpT and BpT chelators includes cellular iron deprivation, resulting in the inhibition of ribonucleotide reductase (RR), which catalyzes the rate-limiting step of DNA synthesis (Merlot et al., 2012). More recently, chelators from these classes, namely Dp44mT and 2-benzoylpyridine-4,4-dimethyl-3-thiosemicarbazone, were shown to have an additional mechanism of RR inhibition *via* their effects on major thiol-containing systems (Yu et al., 2011b). Additionally, these ligands modulate the expression of a variety of proteins involved in cell cycle control, such as members of the cyclin family and cyclin-dependent kinases (Yu et al., 2007). Another significant mode of action is the up-regulation of the growth and metastasis suppressor protein, N-myc downstream regulated gene-1 (NDRG1) (Kovacevic et al., 2011a), which has been shown to be critically important in the progression and outcome of a variety of neoplasms (Bandyopadhyay et al., 2003; Bandyopadhyay et al., 2004; Guan et al., 2000; Hosoi et al., 2009).

Recently, deferasirox was reported to inhibit the growth of myeloid leukemia cells *in vitro* and *in vivo* (Ohyashiki et al., 2009). Moreover, deferasirox was shown to induce a complete remission in a patient suffering chemotherapy-resistant acute monocytic leukemia (Fukushima et al., 2011). Hence, considering its oral activity, low toxicity and demonstrated anti-proliferative effects, deferasirox may have potential applications in cancer treatment. However, there have been no studies that have assessed the ability of deferasirox to inhibit the growth of solid human tumors *in vivo*. Additionally, its mechanism of action remains poorly understood. Hence, further *in vitro* and *in vivo* studies examining this compound are required to fully elucidate its anti-tumor activity.

Herein, we investigate for the first time, the *in vivo* activity of deferasirox against solid human tumor xenografts. We also investigate the *in vitro* activity of deferasirox against human DMS-53 small cell lung carcinoma and SK-N-MC neuroepithelioma cells, and dissect its molecular mechanism of action by examining its effect on the expression of molecules involved in cellular iron metabolism, tumor metastasis and cell cycle control.

Materials and Methods

Cell Culture

The human DMS-53 small cell lung carcinoma and SK-N-MC neuroepithelioma cell lines were obtained from the American Type Culture Collection (Manassas, VA, USA). The DMS-53 and SK-N-MC cells were cultured in RPMI and DMEM media (Life Technologies, Carlsbad, CA), respectively. Media were supplemented with 10% (v/v) fetal calf serum (FCS), L-glutamine (2 mM), penicillin (100 U/mL), streptomycin (100 µg/mL), non-essential amino acids (0.1 mM) and sodium pyruvate (1 mM; all supplements from Life Technologies) using standard techniques, as described previously (Whitnall et al., 2006). All cells were incubated at 37°C in a humidified atmosphere containing 5% CO₂. Experiments were performed when the cultures were approximately 80% confluent.

Chelators

The base of the ligand, Dp44mT, was synthesized and characterized using standard procedures (Whitnall et al., 2006; Yuan et al., 2004). Desferrioxamine (DFO) and deferasirox (Exjade[®]) were obtained from Novartis (Basel, Switzerland). Both Dp44mT and deferasirox were dissolved in dimethyl sulfoxide at a stock concentration of 10 mM and were used at the concentrations indicated in the *Results* section and figures by dilution in culture media containing 10% FCS. For *in vivo* studies, deferasirox was dissolved at a stock concentration of 8.2 mM in sodium chloride solution (0.9% w/v; Baxter Healthcare, Australia). The DFO was dissolved directly in culture media.

Cellular Proliferation Assay

The well-established 3-(4,5-dimethylthiazol)-2,5-diphenyl tetrabromide (MTT) assay was used to assess cell proliferation (Richardson et al., 1995). The cells were incubated with Dp44mT, DFO and deferasirox for 72 h/37°C. Formazan product formation was shown to be directly proportional to viable cell counts (Richardson et al., 1995).

Preparation of ⁵⁹Fe-Transferrin

Human transferrin (Tf; Sigma Aldrich, NSW, Australia) was labeled with ⁵⁹Fe (Perkin Elmer, Boston, USA) to produce ⁵⁹Fe₂-Tf (⁵⁹Fe-Tf), as previously reported (Richardson and Baker, 1992).

⁵⁹Fe Efflux from SK-N-MC and DMS-53 Cells

Iron efflux experiments examining the ability of various chelators to mobilize ⁵⁹Fe from SK-N-MC and DMS-53 cells were performed using established techniques (Baker et al., 1992; Richardson et al., 1995). Briefly, following pre-labeling of cells with ⁵⁹Fe-Tf (0.75 μM) for 3 h/37°C, the cultures were washed four times on ice with ice-cold PBS and subsequently re-incubated for 3 h at 37°C with each chelator (25 and 50 μM) or medium alone (control). The overlying media containing released ⁵⁹Fe was then separated from the cells and placed into γ-counting tubes. The cells were then removed from the plate in 1 mL of PBS using a plastic spatula and placed into a separate set of γ-counting tubes. Radioactivity was measured in both the cell pellet and supernatant using a γ-scintillation counter (Wizard 1480 3"; PerkinElmer-Wallac, Turku, Finland).

Effect of Chelators at Preventing ^{59}Fe Uptake from Tf

The ability of the chelators to prevent cellular ^{59}Fe uptake from ^{59}Fe -Tf was examined using standard techniques (Becker and Richardson, 1999; Yuan et al., 2004). Briefly, SK-N-MC or DMS-53 cells were incubated with ^{59}Fe -Tf (0.75 μM) for 3 h/37°C in the presence of each of the chelators (50 μM) or the medium alone (control). The cells were then washed four times on ice with ice-cold PBS and internalized ^{59}Fe was determined by placing the culture plates on ice and incubating the cell monolayer with the general protease, Pronase (1 mg/mL; Sigma), for 30 min/4°C (Richardson and Baker, 1992). The cells were then removed from the monolayer using a plastic spatula and centrifuged for 1 min at 14,000 rpm. The resulting supernatant represented membrane-bound ^{59}Fe -Tf that was released by the protease, while the internalized ^{59}Fe in the cell pellet was the pronase-insensitive fraction (Baker et al., 1992). The fractions were placed in different γ -counting tubes and the radioactivity measured using the γ -scintillation counter described above.

Tumor Xenografts in Nude Mice and Deferasirox Administration

All animal experiments were performed according to the Australian Code of Practice for the Care and Use of Animals for Scientific Purposes and approved by The University of Sydney Animal Care and Ethics Committee. Female BALB/c (nu/nu) mice were purchased from the Animal Resources Centre (Canning Vale, Perth, WA, Australia) and were housed in sterile conditions. Experiments commenced when the mice were 8-10 weeks of age. Tumor cells (DMS-53) in culture were harvested and re-suspended in a 1:1 ratio of RPMI and Matrigel TM (BD Biosciences, San Jose, CA). Viable cells (5×10^6 cells) were injected subcutaneously into the right flanks of mice. After engraftment, tumor size was measured by Vernier calipers every 2

days. When tumor volumes reached 120 mm³, oral treatment began (day 0). Each group of mice ($n=6$) received deferasirox suspended in saline which was administered by oral gavage every second day, with 3 treatments/week, over 18 days at 20 or 40 mg/kg. Control mice were treated with vehicle alone. At the end of the experiment, the animals were sacrificed and the tumors were excised, weighed and further processed for histological and biochemical analysis (Yu et al., 2011a).

Tissue Iron, Copper and Zinc Determination

Tissue non-heme iron, copper and zinc concentrations were measured using inductively coupled plasma atomic emission spectrometry (ICP-AES) using standard techniques (Yu et al., 2011a).

Hematology, Serum Biochemistry and Histology

At the end of the experiment, mice were anaesthetized with isoflurane and blood samples were collected by cardiac puncture. Hematological parameters as well as serum biochemistry were then determined using a Konelab 20i analyzer (Thermo-Electron Corporation, Vantaa, Finland) and Sysmex K-4500 analyzer (TOA Medical Electronics Co., Kobe, Japan), respectively (Rahmanto and Richardson, 2009). Dissected organs were fixed in 10% formalin, sectioned and stained with hematoxylin and eosin (H & E), Perls' or Gomori trichrome for microscopic examination.

Western Blotting

After 24 h/37°C incubation of cells with control medium or this medium containing the chelators, protein was extracted from whole cells and concentration measured using standard protocols (Gao and Richardson, 2001). Protein samples (30 µg/lane) were separated on a 4-12%

NuPage Bis-Tris gel (Life Technologies) and transferred to a polyvinylidene difluoride membrane (Life Technologies) according to the manufacturer's protocol. The following primary antibodies were used: goat anti-human NDRG1 (Cat. #: ab37897; Abcam, Cambridge, MA, USA), mouse monoclonal anti-human transferrin receptor-1 (TfR1; Cat.#: 136800; Life Technologies), mouse anti-human cyclin D1 (Cat. #: SC-8396; Santa Cruz, CA, USA), rabbit anti-human p21^{CIP1/WAF1} (Cat. #: 2947; Cell Signaling, MA, USA), rabbit anti-human cleaved poly (ADP-ribose) polymerase-1 (PARP1; Cat. #: 9541; Cell Signaling), rabbit anti-human cleaved caspase-3 (Cat. #: 9664; Cell Signaling) and β -actin (Cat. #: SC-130301; Santa Cruz). All primary antibodies were used at a 1:1,000 dilution, except NDRG1 (1:2,000) and β -actin (1:10,000). All secondary antibodies (Sigma Aldrich) were used at a 1:10,000 dilution.

Membranes were probed for β -actin as a loading control and all sample data values were normalized to the corresponding β -actin data values. Densitometric analysis was performed using Quantity One 1D-Analysis software (Bio-Rad, Hercules, CA).

Statistical Analysis

Data are expressed as mean \pm S.E.M. Data were compared against the respective control in each experiment using Student's *t*-test. Results were considered statistically significant when $p < 0.05$.

Results

In vitro anti-proliferative activity of deferasirox against solid tumor cells

We examined the *in vitro* anti-proliferative activity of deferasirox against the DMS-53 lung carcinoma and SK-N-MC neuroepithelioma tumor cell lines using the MTT proliferation assay. The SK-N-MC and DMS-53 cell lines were chosen as the anti-proliferative activity of the chelator, Dp44mT, has been well characterized in these cells both *in vitro* and *in vivo* (Whitnall et al., 2006; Yuan et al., 2004). The well described chelators, DFO (Kalinowski and Richardson, 2005) and Dp44mT (Whitnall et al., 2006), were included in these studies to provide appropriate positive controls.

Deferasirox showed anti-proliferative activity against DMS-53 lung carcinoma cells that was similar to that found for DFO (Table 1, Figure 2). However, deferasirox showed slightly less anti-proliferative efficacy than DFO using the SK-N-MC neuroepithelioma cell line (IC_{50} : 14 ± 2 μ M and 10 ± 1 μ M, respectively; Table 1, Figure 2). The activity of deferasirox in these cell lines was at least 1,400-fold lower when compared to the potent thiosemicarbazone chelator, Dp44mT (Table 1, Figure 2). In agreement with previous studies, the activity (IC_{50}) of DFO was at least 1000-fold lower than Dp44mT in SK-N-MC and DMS-53 cells (Whitnall et al., 2006). The more potent activity of Dp44mT in these cells may reflect enhanced membrane permeability relative to DFO and deferasirox (Kalinowski and Richardson, 2005).

Iron efflux and uptake studies

Considering the link between anti-proliferative activity and iron chelation (Richardson et al., 1995), we next examined the ability of deferasirox to remove iron from cells pre-labeled with ^{59}Fe and to prevent the uptake of iron from ^{59}Fe labeled transferrin (Tf) using standard protocols (Lovejoy and Richardson, 2002; Richardson et al., 1995). To provide appropriate positive controls, we included the chelators, DFO and Dp44mT, which have been well characterized in previous iron efflux and uptake studies (Lovejoy and Richardson, 2002; Richardson et al., 1995).

The current studies showed that in terms of iron efflux, deferasirox was slightly more effective than DFO (Figure 3A), although both these chelators exhibited moderate iron chelation efficacy relative to the highly active lipophilic chelator Dp44mT. Specifically, Dp44mT (25 and 50 μM) was able to efflux approximately 50% of cellular ^{59}Fe from SK-N-MC cells after a 3 h incubation with ^{59}Fe -Tf, whereas DFO and deferasirox were only able to efflux 18% and 36% cellular ^{59}Fe at 50 μM , respectively (Figure 3A). Similar results were obtained using the DMS-53 lung carcinoma cell line, where 50 μM DFO, deferasirox and Dp44mT mobilized 41%, 44% and 66% of cellular ^{59}Fe , respectively (Figure 3B). For both cell-types, the chelator-mediated ^{59}Fe mobilization was significantly ($p < 0.001-0.01$) greater than that found for control medium alone.

Using SK-N-MC cells, deferasirox was more active than DFO in terms of preventing ^{59}Fe uptake, limiting it to 40% of the control at 50 μM , whereas DFO was only able to limit ^{59}Fe uptake to 80% of the control in these cells (Figure 3C). Again, Dp44mT was most active, reducing ^{59}Fe uptake to approximately 5% of the control at 25 μM and 50 μM . However, in DMS-53 cells, DFO and deferasirox reduced ^{59}Fe uptake to a similar extent, 41% and 42%,

respectively (Figure 3D), whereas Dp44mT was able to limit ^{59}Fe uptake to 3% of the control. These studies again confirm the greater iron chelation efficacy of Dp44mT compared to both DFO and deferasirox and for all ligands the decrease in ^{59}Fe uptake was significantly ($p < 0.001$ - 0.01) different to the control.

Effect of deferasirox on the growth of human lung carcinoma xenografts

Considering the demonstrated *in vitro* anti-proliferative activity of deferasirox (Figure 2; Table 1), we next examined if deferasirox could inhibit the growth of DMS-53 lung carcinoma tumor xenografts in BALB/c nude mice. As deferasirox is given to patients orally (in tablet form), we administered deferasirox as a saline suspension by oral gavage in accordance with previous studies (Sato et al., 2011). Initially, we attempted to define a maximum tolerated dose (MTD) to determine an optimal treatment regimen. In fact, we were unable to reach MTD weight loss criteria with increasing dose, with no weight loss occurring in mice even after a 200 mg/kg dose every second day, 3 treatments/week for 4 weeks. However, since a 20 mg/kg/day regimen is considered effective and well-tolerated in patients with iron overload (Nisbet-Brown et al., 2003), we reasoned that 20 mg/kg and 40 mg/kg could be appropriate initial doses to examine in these tumor xenograft studies. Indeed, a preliminary tumor growth experiment in mice suggested that a 20 mg/kg dose markedly suppressed tumor growth (data not shown). Significantly, to minimize effects on systemic iron levels in the mice, deferasirox was only administered once every second day.

In a more comprehensive DMS-53 lung carcinoma tumor study in mice, deferasirox administered orally at 20 and 40 mg/kg (every second day, 3 treatments/week for 18 days) resulted in marked inhibition of tumor growth as determined by measurements of tumor volume

and tumor weight (Figure 4A, B). After 18 days of oral treatment with the vehicle control (saline solution), the tumor xenografts reached an average volume of $1095 \pm 85 \text{ mm}^3$. In contrast, tumor volume was significantly ($p < 0.01$) reduced to 424 ± 100 and $517 \pm 80 \text{ mm}^3$ in mice treated with 20 and 40 mg/kg deferasirox, respectively (Figure 4A). These final tumor volumes after 18 days of treatment were consistent with weights of excised tumors post necropsy. In fact, control tumors weighed $1.3 \pm 0.1 \text{ g}$, while tumors treated with 20 and 40 mg/kg of oral deferasirox weighed significantly ($p < 0.01$) less than control tumors, being $0.5 \pm 0.2 \text{ g}$ and $0.6 \pm 0.2 \text{ g}$, respectively (Figure 4B).

Toxicological effects of oral deferasirox treatment in tumor bearing mice

Treatment with deferasirox, given at 20 or 40 mg/kg over an 18 day treatment period, did not cause any significant ($p > 0.05$) loss of body weight in the mice (Figure 4C), nor were weights of the liver, spleen, kidney, heart, brain or lung significantly affected (Table 2). Examination of hematological indices showed no significant alterations in white or red blood cell count, hemoglobin or hematocrit (Table 3). Platelet counts were slightly elevated in the deferasirox-treatment groups, but this was not statistically significant (Table 3). Additionally, there were no significant changes in biochemical indices in deferasirox-treated mice compared to the control group (Table 3). These data suggested that oral deferasirox treatment at 20 and 40 mg/kg was well tolerated over the treatment period.

Organ Histology

Major organs from control- and deferasirox-treated mice were also taken for histopathological examination (Supplementary Figure 1). Past studies examining the anti-cancer chelators

Triapine[®] and Dp44mT in mice showed that Triapine[®] increased the number of hematopoietic cells in the splenic red pulp (Whitnall et al., 2006). Moreover, at high non-optimal doses Dp44mT induced cardiac fibrosis as demonstrated by Gomori trichrome staining of cardiac sections (Whitnall et al., 2006). Additionally, another study demonstrated that the chelator, Bp44mT, induced cytoplasmic vacuolation in the liver of mice thereby increasing the weight of the organ, although use of a recovery group of mice showed that these effects were partly reversible (Yu et al., 2011a). Hence, we carefully assessed tissue sections for evidence of these and other abnormalities. Significantly, there was no marked alteration in the number of hematopoietic cells in spleens from deferasirox-treated mice compared to control spleens (Supplementary Figure 1). This agreed with Perls' stained spleen sections which indicated no alteration in hemosiderin derived from macrophages generally present in the splenic red pulp of normal mice (Suttie, 2006; Yu et al., 2011a), or the presence of other splenic iron deposits in deferasirox-treated mice compared to controls (Supplementary Figure 1).

There was also no cytoplasmic vacuolation of the liver or evidence of necrosis or fibrosis in the livers of deferasirox-treated mice compared to the vehicle control (Supplementary Figure 1). This was again consistent with the finding that liver weights did not increase in the deferasirox treated groups (Table 2). Additionally, there was no cardiac fibrosis or other abnormalities detected in hearts from deferasirox-treated mice compared to control hearts (Supplementary Figure 1). All other H&E stained sections including those from the kidney, lung and brain appeared normal (data not shown). These data agreed with the lack of change in the weights of these organs in deferasirox-treated and control groups (Table 2).

Total tissue iron, copper and zinc levels

Although deferasirox binds ferric iron with high affinity and selectivity, its ability to transiently lower plasma copper and zinc has been noted (Steinhauser et al., 2004). Hence, we quantified all three of these metals using ICP-AES in liver, kidney and tumor tissue excised from deferasirox- and vehicle control-treated mice. No significant ($p>0.05$) difference in iron levels between the deferasirox and control groups was observed in the liver, kidney or tumor (Supplementary Table 1). However, deferasirox at both 20 and 40 mg/kg significantly ($p<0.05$) increased the copper levels in the kidney relative to untreated controls (Supplementary Table 1). Copper content was also significantly ($p<0.05$) elevated in tumors from the 40 mg/kg deferasirox-treated group (Supplementary Table 1). However, copper levels in the livers of deferasirox-treated mice were similar to those of the control group.

In terms of zinc concentration, there were no significant ($p>0.05$) changes in the livers or kidneys of deferasirox-treated mice relative to the control (Supplementary Table 1). However, zinc levels in tumors from the 20 mg/kg deferasirox-treated group were significantly ($p<0.05$) lower than the control. While zinc levels were also lower in the 40 mg/kg deferasirox-treated group, it was not significantly ($p>0.05$) lower than the control level (Supplementary Table 1).

Deferasirox regulates the expression of the iron-regulated proteins, TfR1 and NDRG1, and also proteins involved in cell cycle control, namely p21^{CIP1/WAF1} and cyclin D1

Iron is involved in cell cycle progression by modulating the expression of molecules involved in cell cycle control, including p21^{CIP1/WAF1} and cyclin D1 (Fu and Richardson, 2007; Nurtjahja-Tjendraputra et al., 2007). In addition, iron depletion using potent chelators can also up-regulate

the expression of the well known metastasis and growth suppressor, NDRG1 (Kovacevic and Richardson, 2006; Le and Richardson, 2004). Recently, it has been shown that NDRG1 can augment the expression of p21^{CIP1/WAF1} in a variety of cancer cell-types (Kovacevic et al., 2011a), which therefore negatively regulates the cell cycle leading to a G₁/S arrest (Harper et al., 1993). Hence, studies were initiated to assess the effects of deferasirox on the expression of these critical regulators of the cell cycle in comparison to DFO and Dp44mT. As a positive control for cellular iron depletion, we also examined the expression of the TfR1, which is up-regulated under these conditions (Hentze and Kuhn, 1996).

In these studies, cells were incubated with deferasirox (25, 50 and 250 μ M), Dp44mT (5 and 10 μ M) or DFO (25, 50 and 250 μ M) for 24 h/37°C. Notably, lower concentrations of Dp44mT were used as this ligand shows far greater cytotoxic activity than DFO or deferasirox (Table 1; Figure 2). In agreement with previous findings, TfR1 expression was shown to increase significantly ($p < 0.05$) as compared to untreated control cells for all chelator treatments in both cell-types, except for DFO at 25 μ M in DMS-53 cells (Figure 5A, B). This effect is likely a compensatory response to the depletion of iron that is caused by these agents (Kwok and Richardson, 2002).

Assessing total NDRG1 protein expression after incubation with chelators, 2 bands were observed in DMS-53 cells migrating at ~43- and 44-kDa (Figure 5C) which was similar to that previously reported in pancreatic cancer cells (Kovacevic et al., 2011b). However, depending on the chelator and its concentration, 2-3 NDRG1 bands were observed in SK-N-MC cells with 2 bands migrating at ~43- and 44-kDa and a third band migrating at ~45 kDa (Figure 5D). After

incubation with either of the three chelators, there was generally a dose-dependent increase in the ~44 kDa band relative to the control, while for SK-N-MC cells, incubation with 250 μ M DFO or 5 and 10 μ M Dp44mT also led to the appearance of a third NDRG1 band at ~45 kDa (Figure 5D). This third NDRG1 band could also be observed in cells incubated with deferasirox (250 μ M) after over-exposure of the blots (data not shown). It has been suggested that these bands may represent different phosphorylation states of the NDRG1 protein which may play a role in its anti-tumor activity (Kovacevic et al., 2011b; Murakami et al., 2010). Therefore, the up-regulation of NDRG1 may, in part, account for the anti-neoplastic efficacy of these chelators. In addition, our results demonstrate that treating both cell lines with these chelators increased the expression level of p21^{CIP1/WAF1} in a dose-dependent manner compared to control cells (Figure 6A, B).

Cyclin D1 levels have previously been demonstrated to significantly decrease in different cancer cell-types when treated with iron chelators (Nurtjahja-Tjendraputra et al., 2007). In agreement with these studies, our results also demonstrate that DFO, Dp44mT and deferasirox were able to significantly ($p < 0.001-0.05$) reduce cyclin D1 expression in both cell lines examined (Figure 6C, D).

Collectively, these results demonstrate that deferasirox, as well as Dp44mT and DFO, significantly up-regulate the expression of TfR1, NDRG1 and p21^{CIP1/WAF1}, while reducing cyclin D1 levels in DMS-53 and SK-N-MC cell lines.

Deferasirox, as well as Dp44mT and DFO, induces apoptosis in the DMS-53 lung carcinoma and the SK-N-MC neuroepithelioma cell lines

Several studies have demonstrated that the iron chelators, DFO and Dp44mT, can induce apoptosis in a variety of cancer cell lines (Richardson and Milnes, 1997; Yuan et al., 2004). Although the mechanisms by which this occurs remain incompletely understood, DFO has been reported to increase the activity of caspases-3, -8 and -9 (Brard et al., 2006; Wang et al., 2006), while Dp44mT has been shown to increase caspase-3 activity (Yuan et al., 2004), thereby activating apoptosis *via* the mitochondrial/intrinsic pathway. Recent studies have also revealed that deferasirox induces apoptosis in myeloid leukemia cells by targeting caspases (Kim et al., 2011). Iron chelators have also been shown to increase the expression of PARP1, which plays a role in DNA damage detection, repair and cell death pathways (Greene et al., 2002; Kovacevic et al., 2011b; Tang and Porter, 1996).

Considering this, we examined the effect of iron chelators on apoptosis by examining the expression levels of the apoptosis markers, cleaved PARP1 (at ~90 kDa) and cleaved caspase-3 (at ~17 and 19 kDa), in DMS-53 and SK-N-MC solid tumor cells following incubation with either deferasirox or DFO (25, 50 and 250 μ M) and Dp44mT (5 and 10 μ M) for 24 h/37°C. We found that in both cell lines the expression of cleaved PARP1 was significantly ($p<0.05$) increased by these chelators in a concentration-dependent manner (Figure 7A, B). Significant ($p<0.001$) cleavage of caspase-3 was also observed following incubation with 250 μ M deferasirox in DMS-53 cells, but not with lower concentrations of this ligand or with any concentration of DFO or Dp44mT (Figure 7C). In contrast, examining SK-N-MC cells, cleaved caspase-3 was significantly ($p<0.01$) increased after incubation with 250 μ M DFO, 10 μ M

Dp44mT and 250 μ M deferasirox (Figure 7D). In both cell-types, the ~19 kDa caspase-3 band predominated relative to the ~17 kDa band. The difference between the cell lines in terms of the response of apoptotic markers (*e.g.*, cleaved caspase-3) to chelators was notable and has been shown for other apoptotic indicators after incubation of tumor cells with DFO and ligands of the pyridoxal isonicotinoyl hydrazone class (Richardson and Milnes, 1997). This probably reflects the known differences in the molecular mechanisms responsible for the process of cell death in various cell-types. In summary, key molecules involved in the induction of apoptosis were increased after incubation with the chelators, and interestingly, deferasirox was the most active agent in terms of inducing caspase-3 cleavage.

Discussion

Iron chelators currently approved for clinical use, *e.g.*, DFO and deferiprone, have generally demonstrated limited efficacy against tumors *in vivo* (Merlot et al., 2012). For DFO, this is likely due to its hydrophobic nature, short plasma half-life and rapid metabolism (Olivieri and Brittenham, 1997). To date, the reported anti-tumor activity of deferasirox has been limited to leukemia cell models and a hepatoma cell line *in vitro* (Lescoat et al., 2007; Ohyashiki et al., 2009). Herein, we investigated, for the first time, the *in vivo* activity of deferasirox against solid human tumor xenografts. We also assessed the *in vitro* efficacy of deferasirox and the molecular mechanism of action underlying its anti-proliferative effects relative to other well described ligands.

We observed that the anti-proliferative activity of deferasirox was similar to DFO in DMS-53 cells and slightly lower compared to DFO in SK-N-MC cells (Table 1, Figure 2). Considering the link between anti-proliferative activity and iron chelation, we also examined the ability of deferasirox to remove iron from cells and prevent iron uptake from Tf. We found that deferasirox was generally similar or slightly more effective than DFO at mobilizing ⁵⁹Fe depending on the cell-type and that both these chelators were far less effective than the highly cytotoxic chelator, Dp44mT (Figure 3). Similarly, deferasirox and DFO showed similar efficacy at inhibiting iron uptake from Tf, but again, were far less effective than Dp44mT. Therefore, the ability of deferasirox to inhibit solid tumor cell growth *in vitro* may be due, at least in part, to its ability to bind and mobilize cellular iron that is vital for replication.

Given the *in vitro* anti-proliferative activity of deferasirox and its efficacy at chelating cellular iron, we then examined its activity on the growth of tumor xenografts in nude mice. Studies *in vivo* found a marked inhibition of DMS-53 tumor xenograft growth in mice treated with 20 and 40 mg/kg deferasirox by oral gavage after 18 days (Figure 4A, B). Considering the high efficacy of deferasirox against DMS-53 xenografts, it was important to examine any potential toxic side effects. By the last day of treatment, we noted no significant loss of body weight (Figure 4C), nor significant alterations to white or red blood cell count, hemoglobin, hematocrit or platelet count (Table 3). Additionally, no significant changes in biochemical indices were observed, suggesting that oral deferasirox was well tolerated.

In terms of the anti-tumor effect observed *in vivo*, there was no significant decrease in tumor iron levels, which correlated with the lack of alteration in hematological and serum biochemical indices at the deferasirox doses implemented. Previous studies have reported that deferasirox at similar doses [*i.e.*, 30 mg/kg/day for 8 weeks (Nick et al., 2009) or 10 mg/kg twice every day or every other day for 7 days (Ibrahim et al., 2007)] also did not significantly alter tissue iron levels, hematological indices, or serum biochemical indices in mice. The observations in our study showing little effect on normal tissue or tumor iron levels could be related to the low doses of the chelator used (20 and 40 mg/kg) and also the short treatment duration (18 days). Considering the lack of a significant effect of deferasirox on tumor iron levels, the marked effect on tumor growth was surprising. This may be explained by the formation of the deferasirox iron complex within the tumor that is not effluxed due to its increased hydrophobicity. The formation of an intracellular iron complex with deferasirox would prevent the utilization of iron for tumor cell proliferation. However, this explanation does not correlate with the effect of deferasirox in cell

culture, where it induced iron efflux and inhibited iron uptake (Figure 3). This may potentially reflect the well known differences in the tumor cell microenvironment *in vitro* and *in vivo*. Similar observations have also been reported for thiosemicarbazone chelators *in vivo*, where substantially lower doses markedly inhibited tumor growth, but had little effect on tumor iron levels (Whitnall et al., 2006; Yu et al., 2011a). For these latter ligands, this effect could lead to tumor cytotoxicity due to the redox activity of these complexes (Whitnall et al., 2006; Yu et al., 2011a). However, this could not explain the anti-tumor efficacy of deferasirox, as its Fe complex is not redox active (Bendová et al., 2010; Hašková et al., 2011).

Another important outcome of the current study was that oral deferasirox demonstrated no significant histopathology in major organs. We observed no cytoplasmic vacuolation of the liver or evidence of necrosis or fibrosis, as well as no cardiac fibrosis (Supplementary Figure 1). This finding agreed with Perls'-stained spleen sections, which indicated no alteration in hemosiderin levels. Further, we quantified total tissue iron, copper and zinc levels in liver, kidney and tumor tissue and found no significant difference in iron levels between mice treated with deferasirox and the vehicle. Hence, deferasirox did not affect normal systemic or tumor iron metabolism. However, deferasirox increased kidney copper levels at both 20 and 40 mg/kg and at the highest dose there was almost a two-fold increase in tumor copper. In contrast, deferasirox had no effect on zinc levels in normal tissues, but reduced zinc in the tumor at both doses and this was significant at 20 mg/kg (Supplementary Table 1). The significant increase in copper in the kidney upon deferasirox treatment may reflect filtration of the copper-deferasirox complex and subsequent trapping within the organ, potentially due to the greater lipophilicity of the complex. The increase in copper, but decrease in zinc in the tumor in the absence of alterations in iron

levels is intriguing. These observations could reflect perturbations in metal metabolism mediated by deferasirox that could inhibit tumor growth. Indeed, like iron, zinc is also necessary for proliferation (Merlot et al., 2012) and its depletion could lead to the decreased tumor growth *in vivo* after deferasirox treatment.

To better characterize the mechanisms involved in the anti-proliferative activity of deferasirox, we investigated its effects on key molecules involved in growth, metastasis, cell cycle regulation and apoptosis. Deferasirox was observed to significantly up-regulate the metastasis suppressor, NDRG1, in both cell-types (Figure 5C, D). This observation is in good agreement with findings with other iron chelators against a variety of cancer cell-types (Le and Richardson, 2004; Whitnall et al., 2006).

We recently demonstrated NDRG1 is able to up-regulate the cyclin-dependent kinase inhibitor, p21^{CIP1/WAF1} (Kovacevic et al., 2011b), which may be important for its tumor-suppressive functions. Here, we further demonstrated that deferasirox and the other chelators also augmented p21^{CIP1/WAF1} expression in DMS-53 lung carcinoma and SK-N-MC neuroepithelioma cells, which may be mediated, in part, by NDRG1 up-regulation. Classically, p21^{CIP1/WAF1} over-expression leads to G₁/S arrest due to its ability to act as a cyclin-dependent kinase inhibitor (Yu et al., 2007). However, the effect of iron chelators on p21^{CIP1/WAF1} expression appears to be cell-type specific or dependent on the ligand utilized (Fu and Richardson, 2007).

We also investigated the expression of the cell cycle regulatory molecule, cyclin D1, following treatment with iron chelators (Yu et al., 2007). Both Dp44mT and DFO significantly reduced

cyclin D1 levels in DMS-53 and SK-N-MC cells (Figure 6C, D), as observed previously (Gao and Richardson, 2001; Nurtjahja-Tjendraputra et al., 2007). Similarly, we also showed that deferasirox was able to significantly decrease cyclin D1 levels. It is notable that in a number of cancer cell-types, over-expression of cyclin D1 is correlated with poor patient survival (Kornmann et al., 1998; Mishina et al., 1999). Consequently, the ability of iron chelators, including deferasirox, to reduce cyclin D1 levels could be important for their anti-proliferative effects.

Considering the alterations in the expression of proteins involved in cell metabolism and cell cycle control, we then investigated the effect of deferasirox on molecules involved in mediating apoptosis, namely cleaved PARP1 and cleaved caspase-3. We demonstrated deferasirox was able to significantly induce cleavage of PARP1 and caspase-3 in DMS-53 and SK-N-MC cells. These observations in cells from solid tumors agree with similar results in leukemia cells (Kim et al., 2011). These findings indicate that this agent is able to induce apoptosis, further supporting the potential of deferasirox as an agent for cancer treatment. Finally, since the combination of chelators with current chemotherapeutics can significantly enhance cytotoxicity (Lovejoy et al., 2012; Messa et al., 2010), the potential for deferasirox to be used in combination with established cytotoxics is also promising.

In summary, this study is the first to examine the *in vivo* anti-tumor activity of deferasirox against human cancer cells from solid tumors. Importantly, we observed that deferasirox inhibited the growth of DMS-53 tumor xenografts, while having no significant toxic side-effects. We also demonstrated that deferasirox displayed anti-proliferative effects *in vitro* in DMS-53

and SK-N-MC cells. At the molecular level, deferasirox up-regulated the expression of NDRG1 and p21^{CIP/WAF1} and down-regulated cyclin D1, which are key molecules involved in tumor growth, metastasis and cell cycle control. Moreover, deferasirox also up-regulated the expression of the apoptosis markers, cleaved PARP1 and cleaved caspase-3. Collectively, these results indicate deferasirox is an effective and selective iron chelator with potential as an orally-active chemotherapeutic.

Acknowledgments:

The authors thank Dr. Christopher Austin, Dr. Katie Dixon, Dr. Yu Yu, Dr. Darius Lane, Ms. Angelica Merlot, Dr. Vera Richardson and Dr. Daohai Zhang of the Iron Metabolism and Chelation Program (University of Sydney) for their critical appraisal of the manuscript prior to submission.

Authorship Contributions:

Participated in research design: Lui, Obeidy, Ford, Lovejoy, Kovacevic, Jansson, Tselepis and Richardson.

Conducted experiments: Lui, Obeidy and Sharp.

Contributed new reagents or analytic tools: Obeidy, Lovejoy and Richardson.

Performed data analysis: Lui, Obeidy, Lovejoy, Kovacevic and Richardson.

Wrote or contributed to the writing of the manuscript: Lui, Obeidy, Lovejoy, Kalinowski, Kovacevic and Richardson.

References

- Baker E, Richardson D, Gross S and Ponka P (1992) Evaluation of the iron chelation potential of hydrazones of pyridoxal, salicylaldehyde and 2-hydroxy-1-naphthylaldehyde using the hepatocyte in culture. *Hepatology* **15**(3): 492-501.
- Bandyopadhyay S, Pai SK, Gross SC, Hirota S, Hosobe S, Miura K, Saito K, Commes T, Hayashi S, Watabe M and Watabe K (2003) The Drg-1 gene suppresses tumor metastasis in prostate cancer. *Cancer Res* **63**(8): 1731-1736.
- Bandyopadhyay S, Pai SK, Hirota S, Hosobe S, Takano Y, Saito K, Piquemal D, Commes T, Watabe M, Gross SC, Wang Y, Ran S and Watabe K (2004) Role of the putative tumor metastasis suppressor gene Drg-1 in breast cancer progression. *Oncogene* **23**(33): 5675-5681.
- Becker E and Richardson DR (1999) Development of novel aroylhydrazone ligands for iron chelation therapy: 2-pyridylcarboxaldehyde isonicotinoyl hydrazone analogs. *J Lab Clin Med* **134**(5): 510-521.
- Bendová P, Macková E, Haškova P, Vávrová A, Jirkovský E, Štěřba M, Popelová O, Kovaříková P, Vávrová K, Ponka P, Richardson DR and Simůnek T (2010) Comparison of clinically used and experimental iron chelators for protection against oxidative stress-induced cellular injury. *Chem Res Toxicol* **23**(6): 1105-1114.
- Brard L, Granai CO and Swamy N (2006) Iron chelators deferoxamine and diethylenetriamine pentaacetic acid induce apoptosis in ovarian carcinoma. *Gynecol Oncol* **100**(1): 116-127.
- Broto P, Moreau G and Vandycke C (1984) Molecular structures: perception, autocorrelation descriptor and SAR studies. System of atomic contributions for the calculation of the n-octanol/water partition coefficients. *Eur J Med Chem* **19**: 71-78.
- Cappellini MD (2007) Exjade(R) (deferasirox, ICL670) in the treatment of chronic iron overload associated with blood transfusion. *Ther Clin Risk Manag* **3**(2): 291-299.
- Chaston TB, Lovejoy DB, Watts RN and Richardson DR (2003) Examination of the antiproliferative activity of iron chelators: multiple cellular targets and the different mechanism of action of Triapine compared with desferrioxamine and the potent pyridoxal isonicotinoyl hydrazone analogue 311. *Clin Cancer Res* **9**(1): 402-414.
- Chua AC, Graham RM, Trinder D and Olynyk JK (2007) The regulation of cellular iron metabolism. *Crit Rev Clin Lab Sci* **44**(5-6): 413-459.

- Finkenstedt A, Wolf E, Hofner E, Gasser BI, Bosch S, Bakry R, Creus M, Kremser C, Schocke M, Theurl M, Moser P, Schranz M, Bonn G, Poewe W, Vogel W, Janecke AR and Zoller H (2010) Hepatic but not brain iron is rapidly chelated by deferasirox in aceruloplasminemia due to a novel gene mutation. *J Hepatol* **53**(6): 1101-1107.
- Fu D and Richardson DR (2007) Iron chelation and regulation of the cell cycle: 2 mechanisms of posttranscriptional regulation of the universal cyclin-dependent kinase inhibitor p21CIP1/WAF1 by iron depletion. *Blood* **110**(2): 752-761.
- Fukushima T, Kawabata H, Nakamura T, Iwao H, Nakajima A, Miki M, Sakai T, Sawaki T, Fujita Y, Tanaka M, Masaki Y, Hirose Y and Umehara H (2011) Iron chelation therapy with deferasirox induced complete remission in a patient with chemotherapy-resistant acute monocytic leukemia. *Anticancer Res* **31**(5): 1741-1744.
- Gao J and Richardson DR (2001) The potential of iron chelators of the pyridoxal isonicotinoyl hydrazone class as effective antiproliferative agents, IV: The mechanisms involved in inhibiting cell-cycle progression. *Blood* **98**(3): 842-850.
- Ghose AK and Crippen GM (1987) Atomic physicochemical parameters for three-dimensional-structure-directed quantitative structure-activity relationships. 2. Modeling dispersive and hydrophobic interactions. *J Chem Inf Comput Sci* **27**(1): 21-35.
- Greene BT, Thorburn J, Willingham MC, Thorburn A, Planalp RP, Brechbiel MW, Jennings-Gee J, Wilkinson Jt, Torti FM and Torti SV (2002) Activation of caspase pathways during iron chelator-mediated apoptosis. *J Biol Chem* **277**(28): 25568-25575.
- Guan RJ, Ford HL, Fu Y, Li Y, Shaw LM and Pardee AB (2000) Drg-1 as a differentiation-related, putative metastatic suppressor gene in human colon cancer. *Cancer Res* **60**(3): 749-755.
- Harper JW, Adami GR, Wei N, Keyomarsi K and Elledge SJ (1993) The p21 Cdk-interacting protein Cip1 is a potent inhibitor of G1 cyclin-dependent kinases. *Cell* **75**(4): 805-816.
- Hašková P, Koubková L, Vávrová A, Macková E, Kovaříková P, Vávrová K and Simůnek T (2011) Comparison of various iron chelators used in clinical practice as protecting agents against catecholamine-induced oxidative injury and cardiotoxicity. *Toxicology* **289**: 122-131.
- Hentze MW and Kuhn LC (1996) Molecular control of vertebrate iron metabolism: mRNA-based regulatory circuits operated by iron, nitric oxide, and oxidative stress. *Proc Natl Acad Sci U S A* **93**(16): 8175-8182.

- Hershko C, Konijn AM, Nick HP, Breuer W, Cabantchik ZI and Link G (2001) ICL670A: a new synthetic oral chelator: evaluation in hypertransfused rats with selective radioiron probes of hepatocellular and reticuloendothelial iron stores and in iron-loaded rat heart cells in culture. *Blood* **97**(4): 1115-1122.
- Hosoi F, Izumi H, Kawahara A, Murakami Y, Kinoshita H, Kage M, Nishio K, Kohno K, Kuwano M and Ono M (2009) N-myc downstream regulated gene 1/Cap43 suppresses tumor growth and angiogenesis of pancreatic cancer through attenuation of inhibitor of kappaB kinase beta expression. *Cancer Res* **69**(12): 4983-4991.
- Ibrahim AS, Gebermariam T, Fu Y, Lin L, Hussein MI, French SW, Schwartz J, Skory CD, Edwards JE, Jr. and Spellberg BJ (2007) The iron chelator deferasirox protects mice from mucormycosis through iron starvation. *J Clin Invest* **117**(9): 2649-2657.
- Kalinowski DS and Richardson DR (2005) The evolution of iron chelators for the treatment of iron overload disease and cancer. *Pharmacol Rev* **57**(4): 547-583.
- Kim JL, Kang HN, Kang MH, Yoo YA, Kim JS and Choi CW (2011) The oral iron chelator deferasirox induces apoptosis in myeloid leukemia cells by targeting caspase. *Acta Haematol* **126**(4): 241-245.
- Knox JJ, Hotte SJ, Kollmannsberger C, Winkquist E, Fisher B and Eisenhauer EA (2007) Phase II study of Triapine in patients with metastatic renal cell carcinoma: a trial of the National Cancer Institute of Canada Clinical Trials Group (NCIC IND.161). *Invest New Drugs* **25**(5): 471-477.
- Kornmann M, Ishiwata T, Itakura J, Tangvoranuntakul P, Beger HG and Korc M (1998) Increased cyclin D1 in human pancreatic cancer is associated with decreased postoperative survival. *Oncology* **55**(4): 363-369.
- Kovacevic Z, Chikhani S, Lovejoy DB and Richardson DR (2011a) Novel thiosemicarbazone iron chelators induce up-regulation and phosphorylation of the metastasis suppressor N-myc down-stream regulated gene 1: a new strategy for the treatment of pancreatic cancer. *Mol Pharmacol* **80**(4): 598-609.
- Kovacevic Z and Richardson DR (2006) The metastasis suppressor, NdrG-1: a new ally in the fight against cancer. *Carcinogenesis* **27**(12): 2355-2366.
- Kovacevic Z, Sivagurunathan S, Mangs H, Chikhani S, Zhang D and Richardson DR (2011b) The metastasis suppressor, N-myc downstream regulated gene 1 (NDRG1), upregulates p21 via p53-independent mechanisms. *Carcinogenesis* **32**(5): 732-740.

- Kwok JC and Richardson DR (2002) The iron metabolism of neoplastic cells: alterations that facilitate proliferation? *Crit Rev Oncol Hematol* **42**(1): 65-78.
- Le NT and Richardson DR (2004) Iron chelators with high antiproliferative activity up-regulate the expression of a growth inhibitory and metastasis suppressor gene: a link between iron metabolism and proliferation. *Blood* **104**(9): 2967-2975.
- Lescoat G, Chantrel-Groussard K, Padeloup N, Nick H, Brissot P and Gaboriau F (2007) Antiproliferative and apoptotic effects in rat and human hepatoma cell cultures of the orally active iron chelator ICL670 compared to CP20: a possible relationship with polyamine metabolism. *Cell Proliferat* **40**(5): 755-767.
- Lovejoy DB and Richardson DR (2002) Novel "hybrid" iron chelators derived from aroylhydrazones and thiosemicarbazones demonstrate selective antiproliferative activity against tumor cells. *Blood* **100**(2): 666-676.
- Lovejoy DB, Sharp DM, Seebacher N, Obeidy P, Prichard T, Stefani C, Basha MT, Sharpe PC, Jansson PJ, Kalinowski DS, Bernhardt PV and Richardson DR (2012) Novel second-generation di-2-pyridylketone thiosemicarbazones show synergism with standard chemotherapeutics and demonstrate potent activity against lung cancer xenografts after oral and intravenous administration in vivo. *J Med Chem* **55**(16): 7230-7244.
- Merlot AM, Kalinowski DS and Richardson DR (2012) Novel chelators for cancer treatment: where are we now? *Antioxid Redox Signaling* doi: 10.1089/ars.2012.4540.
- Messa E, Carturan S, Maffe C, Pautasso M, Bracco E, Roetto A, Messa F, Arruga F, Defilippi I, Rosso V, Zanone C, Rotolo A, Greco E, Pellegrino RM, Alberti D, Saglio G and Cilloni D (2010) Deferasirox is a powerful NF-kappaB inhibitor in myelodysplastic cells and in leukemia cell lines acting independently from cell iron deprivation by chelation and reactive oxygen species scavenging. *Haematologica* **95**(8): 1308-1316.
- Mishina T, Dosaka-Akita H, Kinoshita I, Hommura F, Morikawa T, Katoh H and Kawakami Y (1999) Cyclin D1 expression in non-small-cell lung cancers: its association with altered p53 expression, cell proliferation and clinical outcome. *Br J Cancer* **80**(8): 1289-1295.
- Murakami Y, Hosoi F, Izumi H, Maruyama Y, Ureshino H, Watari K, Kohno K, Kuwano M and Ono M (2010) Identification of sites subjected to serine/threonine phosphorylation by SGK1 affecting N-myc downstream-regulated gene 1 (NDRG1)/Cap43-dependent suppression of angiogenic CXC chemokine expression in human pancreatic cancer cells. *Biochem Biophys Res Commun* **396**(2): 376-381.
- Nick H, Allegrini PR, Fozard L, Junker U, Rojkaer L, Salie R, Niederkofler V and O'Reilly T (2009) Deferasirox reduces iron overload in a murine model of juvenile hemochromatosis. *Exp Biol Med (Maywood)* **234**(5): 492-503.

- Nisbet-Brown E, Olivieri NF, Giardina PJ, Grady RW, Neufeld EJ, Sechaud R, Krebs-Brown AJ, Anderson JR, Alberti D, Sizer KC and Nathan DG (2003) Effectiveness and safety of ICL670 in iron-loaded patients with thalassaemia: a randomised, double-blind, placebo-controlled, dose-escalation trial. *Lancet* **361**(9369): 1597-1602.
- Nurtjahja-Tjendraputra E, Fu D, Phang JM and Richardson DR (2007) Iron chelation regulates cyclin D1 expression via the proteasome: a link to iron deficiency-mediated growth suppression. *Blood* **109**(9): 4045-4054.
- Ohyashiki JH, Kobayashi C, Hamamura R, Okabe S, Tauchi T and Ohyashiki K (2009) The oral iron chelator deferasirox represses signaling through the mTOR in myeloid leukemia cells by enhancing expression of REDD1. *Cancer Sci* **100**(5): 970-977.
- Olivieri NF and Brittenham GM (1997) Iron-chelating therapy and the treatment of thalassemia. *Blood* **89**(3): 739-761.
- Porter JB (2009) Optimizing iron chelation strategies in beta-thalassaemia major. *Blood Rev* **23 Suppl 1**: S3-7.
- Rahmanto YS and Richardson DR (2009) Generation and characterization of transgenic mice hyper-expressing melanoma tumour antigen p97 (Melanotransferrin): no overt alteration in phenotype. *Biochim Biophys Acta* **1793**(7): 1210-1217.
- Richardson DR and Baker E (1992) Intermediate steps in cellular iron uptake from transferrin. Detection of a cytoplasmic pool of iron, free of transferrin. *J Biol Chem* **267**(30): 21384-21389.
- Richardson DR and Milnes K (1997) The potential of iron chelators of the pyridoxal isonicotinoyl hydrazone class as effective antiproliferative agents II: the mechanism of action of ligands derived from salicylaldehyde benzoyl hydrazone and 2-hydroxy-1-naphthylaldehyde benzoyl hydrazone. *Blood* **89**(8): 3025-3038.
- Richardson DR, Tran EH and Ponka P (1995) The potential of iron chelators of the pyridoxal isonicotinoyl hydrazone class as effective antiproliferative agents. *Blood* **86**(11): 4295-4306.
- Sato T, Kobune M, Murase K, Kado Y, Okamoto T, Tanaka S, Kikuchi S, Nagashima H, Kawano Y, Takada K, Iyama S, Miyanishi K, Sato Y, Takimoto R and Kato J (2011) Iron chelator deferasirox rescued mice from Fas-induced fulminant hepatitis. *Hepatol Res* **41**(7): 660-667.

- Steinhauser S, Heinz U, Bartholomä M, Weyhermüller T, Nick H and Hegetschweiler K (2004) Complex formation of ICL670 and related ligands with FeIII and FeII. *Eur J Inorg Chem* **2004**(21): 4177-4192.
- Suttie AW (2006) Histopathology of the spleen. *Toxicol Pathol* **34**(5): 466-503.
- Tang DG and Porter AT (1996) Apoptosis: A Current Molecular Analysis. *Pathol Oncol Res* **2**(3): 117-131.
- Viswanadhan VN, Ghose AK, Revankar GR and Robins RK (1989) Atomic physicochemical parameters for three-dimensional-structure-directed quantitative structure-activity relationships. 4. Additional parameters for hydrophobic and dispersive interactions and their application for an automated superposition of certain naturally occurring nucleoside antibiotics. *J Chem Inf Comput Sci* **29**(3): 163-172.
- Wang D, Liu YF and Wang YC (2006) Deferoxamine induces apoptosis of HL-60 cells by activating caspase-3. *Zhongguo Shi Yan Xue Ye Xue Za Zhi* **14**(3): 485-487.
- Whitnall M, Howard J, Ponka P and Richardson DR (2006) A class of iron chelators with a wide spectrum of potent antitumor activity that overcomes resistance to chemotherapeutics. *Proc Natl Acad Sci U S A* **103**(40): 14901-14906.
- Yen Y, Margolin K, Doroshow J, Fishman M, Johnson B, Clairmont C, Sullivan D and Sznol M (2004) A phase I trial of 3-aminopyridine-2-carboxaldehyde thiosemicarbazone in combination with gemcitabine for patients with advanced cancer. *Cancer Chemother Pharmacol* **54**(4): 331-342.
- Yu Y, Kovacevic Z and Richardson DR (2007) Tuning cell cycle regulation with an iron key. *Cell Cycle* **6**(16): 1982-1994.
- Yu Y, Rahmanto YS and Richardson D (2011a) Bp44mT: An orally-active iron chelator of the thiosemicarbazone class with potent anti-tumour efficacy. *Br J Pharmacol* **165**(1): 148-166.
- Yu Y, Suryo Rahmanto Y, Hawkins CL and Richardson DR (2011b) The potent and novel thiosemicarbazone chelators di-2-pyridylketone-4,4-dimethyl-3-thiosemicarbazone and 2-benzoylpyridine-4,4-dimethyl-3-thiosemicarbazone affect crucial thiol systems required for ribonucleotide reductase activity. *Mol Pharmacol* **79**(6): 921-931.
- Yuan J, Lovejoy DB and Richardson DR (2004) Novel di-2-pyridyl-derived iron chelators with marked and selective antitumor activity: in vitro and in vivo assessment. *Blood* **104**(5): 1450-1458.

Footnotes:

G.Y.L.L. and P.O. contributed equally as first authors. D.B.L and Z.K contributed equally as co-senior authors.

This work was supported by the National Health and Medical Research Council of Australia [Project Grant 632778; Senior Principal Research Fellowship 571123]; and the Cancer Institute of New South Wales [Early Career Development Fellowships 07/ECF/1-19, 10/ECF/2-15, 08/ECF/1-30].

Reprint requests to be sent to Prof. Des R. Richardson (Room 555, Blackburn Building D06, University of Sydney, NSW 2006, Australia). Email: d.richardson@med.usyd.edu.au

Figure Legends

Figure 1: Line drawings indicating the chemical structures of: (A) Deferasirox, (B) DFO, (C) 3-AP, and (D) Dp44mT. Log P_{calc} values were the average log P values calculated in ChemDraw v4.5 using Crippen's fragmentation (Ghose and Crippen, 1987), Viswanadhan's fragmentation (Viswanadhan et al., 1989) and Broto's methods (Broto et al., 1984).

Figure 2: Cellular growth assays demonstrating the anti-proliferative activity of deferasirox relative to the well described chelators, Dp44mT and DFO, on DMS-53 lung carcinoma and SK-N-MC neuroepithelioma cells *in vitro*. Cell proliferation was measured using the MTT assay after cells were treated with DFO, Dp44mT or deferasirox over 72 h/37°C. Data are represented as average \pm S.E.M. ($n=3$).

Figure 3: Iron efflux and uptake studies demonstrating the iron chelation efficacy of deferasirox relative to either DFO or Dp44mT in SK-N-MC neuroepithelioma or DMS-53 lung carcinoma cells. The effect of DFO (25 and 50 μM), Dp44mT (25 and 50 μM) or deferasirox (25 and 50 μM) on: **(A, B)** inducing ^{59}Fe efflux over a 3 h/37°C re-incubation period from cells prelabeled with ^{59}Fe -transferrin (0.75 μM) for 3 h/37°C, and **(C, D)** on inhibiting ^{59}Fe uptake from ^{59}Fe -transferrin (0.75 μM) over 3 h/37°C. Results are mean \pm S.E.M. ($n=3$) with 3 replicates in each experiment. For statistical analysis, each treatment was compared to the untreated control; ** vs. control, $p<0.01$ and; *** vs. control, $p<0.001$.

Figure 4: Orally administered deferasirox markedly inhibits the growth of human lung carcinoma xenografts in nude mice. (A) Deferasirox (20 and 40 mg/kg orally; given by gavage every second day, 3 treatments/week, for 18 days) effectively inhibited the growth of human lung carcinoma DMS-53 tumor xenografts *in vivo*. **(B)** Average weights of excised tumors post necroscopy from 20 and 40 mg/kg deferasirox treated mice and mice treated with the vehicle control. **(C)** The average weight of mice in each treatment group during the course of treatment. Data represents average \pm S.E.M ($n=6$ mice/group). For statistical analysis, each treatment was compared to the vehicle control; ** *vs.* control, $p<0.01$.

Figure 5: The effect of deferasirox relative to DFO or Dp44mT on the expression of: (A, B) TfR1, and (C, D) NDRG1 in DMS-53 or SK-N-MC cells. Cells were incubated for 24 h/37°C with either DFO (25, 50 and 250 μ M), Dp44mT (5 and 10 μ M) or deferasirox (25, 50 and 250 μ M) and then the expression levels of TfR1 and NDRG1 were examined using western blotting. The gel photographs are representative of 3-6 experiments, while the densitometric analysis is mean \pm S.E.M ($n=3-6$ experiments). For statistical analysis, each treatment was compared to the untreated control; * *vs.* control, $p<0.05$; ** *vs.* control, $p<0.01$ and; *** *vs.* control, $p<0.001$.

Figure 6: The effect of deferasirox relative to DFO or Dp44mT on the expression of: (A, B) p21^{CIP1/WAF1}, and (C, D) cyclin D1 in DMS-53 or SK-N-MC cells. Cells were incubated for 24 h/37°C with either DFO (25, 50 and 250 μ M), Dp44mT (5 and 10 μ M) or deferasirox (25, 50 and 250 μ M) and then the expression levels of p21^{CIP1/WAF1} and cyclin D1 were examined using western blotting. The gel photographs are representative of 3-6 experiments, while the

densitometric analysis is mean \pm S.E.M ($n=3-6$ experiments). For statistical analysis, each treatment was compared to the untreated control; * *vs.* control, $p<0.05$; ** *vs.* control, $p<0.01$ and; *** *vs.* control, $p<0.001$.

Figure 7: The effect of deferasirox relative to DFO or Dp44mT on the expression of: (A, B) cleaved PARP1 or (C, D) cleaved caspase-3 in DMS-53 or SK-N-MC cells. Cells were incubated with chelators for 24 h/37°C with either DFO (25, 50 and 250 μ M), Dp44mT (5 and 10 μ M) or deferasirox (25, 50 and 250 μ M) and then cleaved PARP1 or cleaved caspase-3 levels were examined using western blotting. The gel photographs are representative of 3-6 experiments, while the densitometric analysis represents mean \pm S.E.M ($n=3-6$ experiments). For statistical analysis, each treatment was compared to the untreated control; * *vs.* control, $p<0.05$; ** *vs.* control, $p<0.01$ and; *** *vs.* control, $p<0.001$.

Table 1: IC₅₀ values (μM) for Dp44mT, DFO and deferasirox after a 72 h/37°C incubation with the DMS-53 lung carcinoma and SK-N-MC neuroepithelioma cell-types. Data represents mean ± S.E.M. (*n*=3).

| | IC ₅₀ (μM) | |
|--------------------|-----------------------|-------------|
| | DMS-53 | SK-N-MC |
| Dp44mT | 0.006 ± 0.003 | 0.01 ± 0.01 |
| DFO | 15 ± 2 | 10 ± 1 |
| Deferasirox | 12 ± 1 | 14 ± 2 |

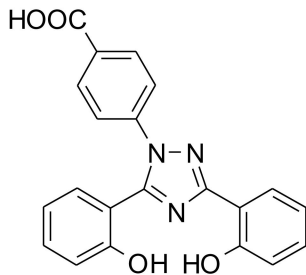
Table 2: Body weight loss (% initial), average tumor and wet organ weights (g) from nude mice bearing a DMS-53 xenograft and treated orally by gavage with the vehicle control or deferasirox (20 or 40 mg/kg; every 2nd day, 3 treatments per week) for 18 days. Values are expressed as mean \pm S.E.M. ($n=6$ mice/group). Statistical analysis was performed using the Student's *t*-test. ** $p<0.01$ vs. control.

| | Treatment Groups | | |
|--------------------------------|-------------------|-------------------|-------------------|
| | Vehicle Control | Deferasirox | |
| | | 20 mg/kg | 40 mg/kg |
| Body weight (% initial) | 112 \pm 2 | 108 \pm 4 | 116 \pm 4 |
| Tumor (g) | 1.3 \pm 0.1 | 0.5 \pm 0.2** | 0.6 \pm 0.2** |
| Liver (g) | 0.86 \pm 0.02 | 0.89 \pm 0.03 | 0.86 \pm 0.03 |
| Spleen (g) | 0.06 \pm 0.01 | 0.07 \pm 0.01 | 0.06 \pm 0.00 |
| Kidney (g) | 0.21 \pm 0.01 | 0.21 \pm 0.01 | 0.18 \pm 0.03 |
| Heart (g) | 0.081 \pm 0.004 | 0.087 \pm 0.003 | 0.083 \pm 0.004 |
| Brain (g) | 0.30 \pm 0.02 | 0.30 \pm 0.02 | 0.31 \pm 0.02 |
| Lung (g) | 0.10 \pm 0.01 | 0.11 \pm 0.01 | 0.11 \pm 0.01 |

Table 3: Hematological and serum indices from nude mice bearing a DMS-53 xenograft and treated orally by gavage with either vehicle control or deferasirox (20 or 40 mg/kg; every 2nd day, 3 treatments per week) for 18 days. Values are expressed as mean \pm S.E.M. Statistical analysis was performed using the Student's *t*-test (*n*=6 mice/group) comparing each treated group to the respective vehicle control.

| | Units | Treatment Groups | | |
|--|---------------------|------------------|-----------------|-----------------|
| | | Vehicle Control | Deferasirox | |
| | | | 20 mg/kg | 40 mg/kg |
| <i>Hematological Indices</i> | | | | |
| Red Blood Cells (RBC) | 10 ¹² /L | 10.7 \pm 0.2 | 10.3 \pm 0.2 | 10.5 \pm 0.2 |
| White Blood Cells (WBC) | 10 ⁹ /L | 3.5 \pm 0.5 | 3.5 \pm 0.5 | 3.7 \pm 0.3 |
| Hemoglobin (HGB) | g/L | 158 \pm 1 | 151 \pm 3 | 155 \pm 2 |
| Hematocrit (HCT) | % | 0.46 \pm 0.01 | 0.44 \pm 0.01 | 0.45 \pm 0.35 |
| Platelets | 10 ⁹ /L | 740 \pm 126 | 822 \pm 104 | 969 \pm 65 |
| <i>Serum Biochemical Indices</i> | | | | |
| Serum Iron | μ mol/L | 32 \pm 2 | 34 \pm 2 | 32 \pm 1 |
| Total Iron-Binding Capacity (TIBC) | μ mol/L | 57 \pm 2 | 60 \pm 3 | 56 \pm 1 |
| Unsaturated Iron-Binding Capacity (UIBC) | μ mol/L | 64 \pm 1 | 63 \pm 3 | 66 \pm 2 |
| Alkaline Phosphatase (ALP) | U/L | 78 \pm 6 | 95 \pm 10 | 93 \pm 5 |
| Alanine Aminotransferase (ALT) | U/L | 58 \pm 8 | 43 \pm 5 | 43 \pm 4 |
| Albumin | g/L | 31.6 \pm 0.8 | 30.3 \pm 0.6 | 30.4 \pm 0.3 |
| Total Protein | g/L | 53 \pm 1 | 57 \pm 3 | 53 \pm 1 |

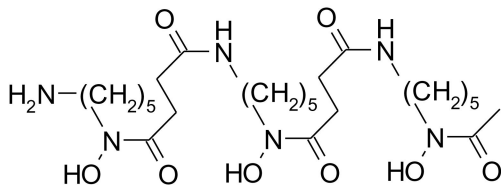
(A)



Deferasirox

$M_r = 373.4$
 $\text{Log } P_{\text{calc}} = 5.16$

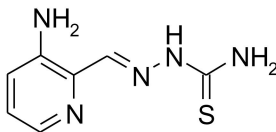
(B)



DFO

$M_r = 560.7$
 $\text{Log } P_{\text{calc}} = -0.49$

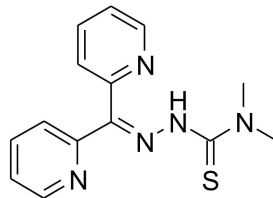
(C)



3-AP

$M_r = 195.3$
 $\text{Log } P_{\text{calc}} = -0.08$

(D)



Dp44mT

$M_r = 285.4$
 $\text{Log } P_{\text{calc}} = 1.98$

Figure 1

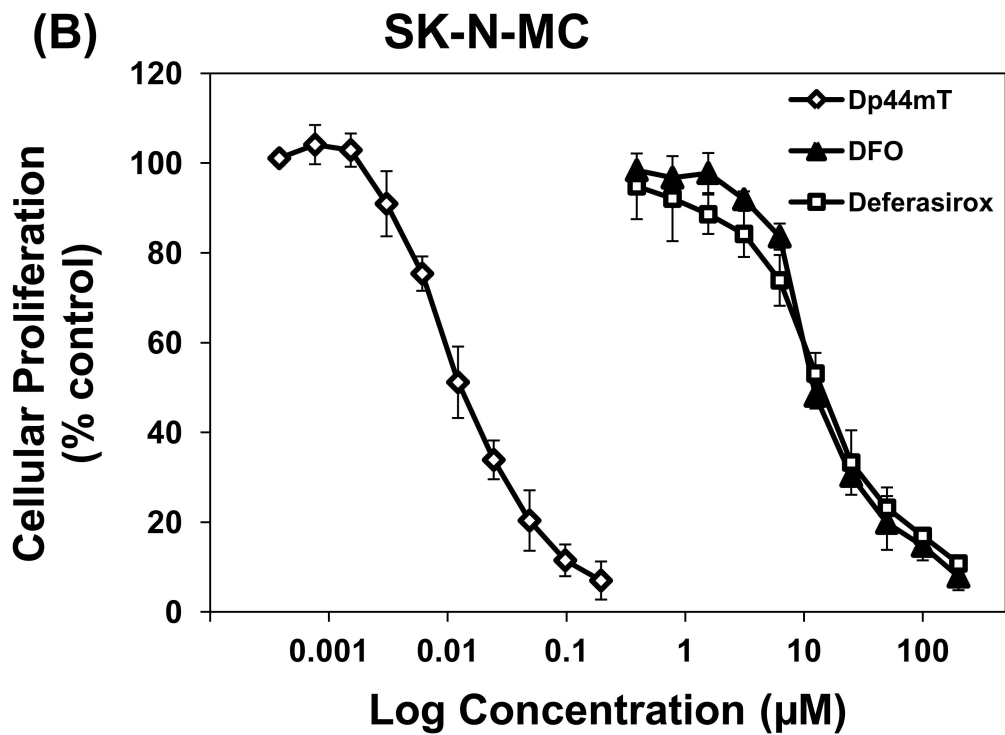
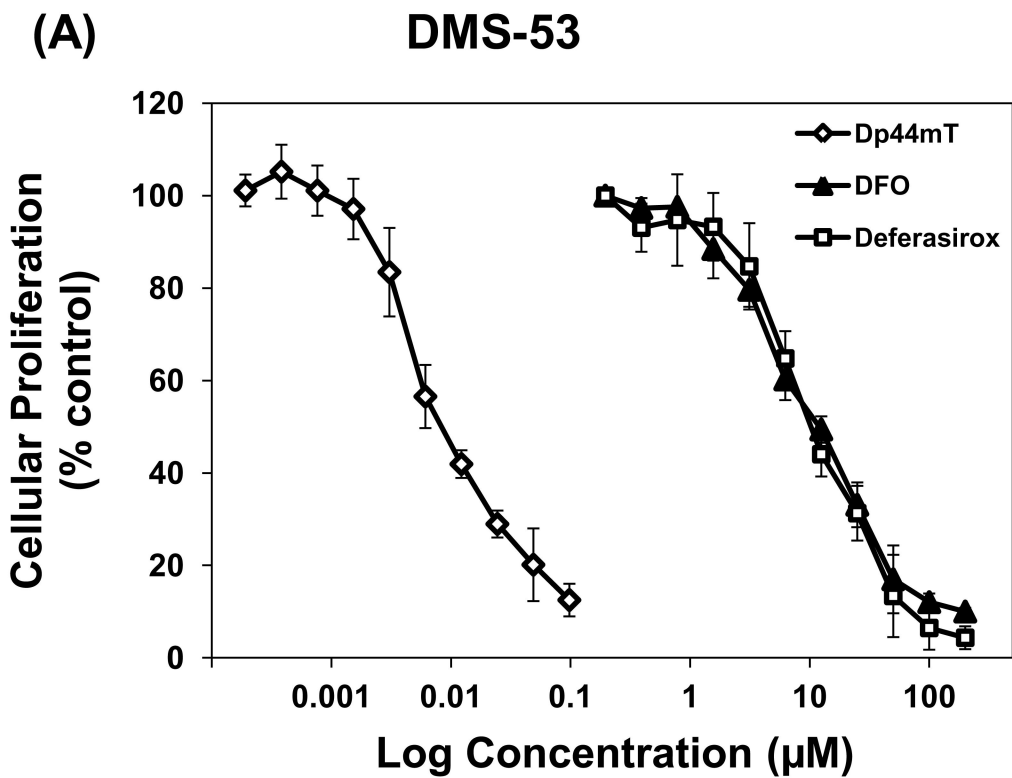


Figure 2

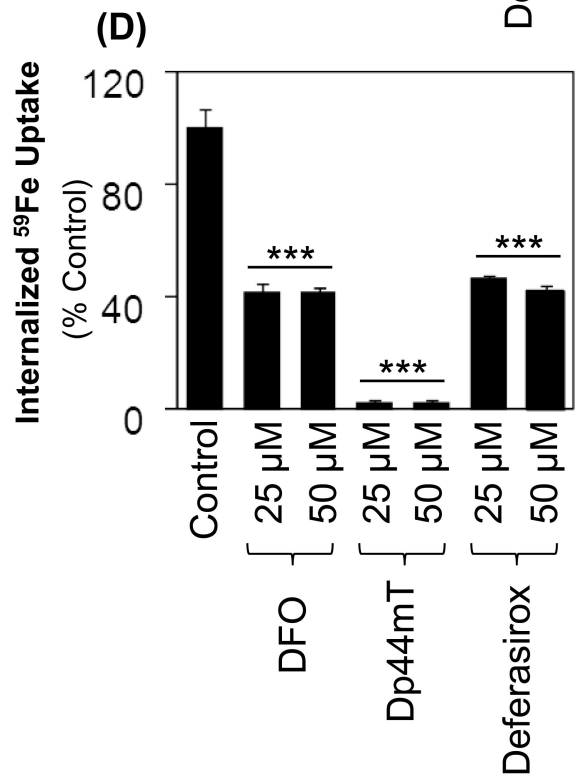
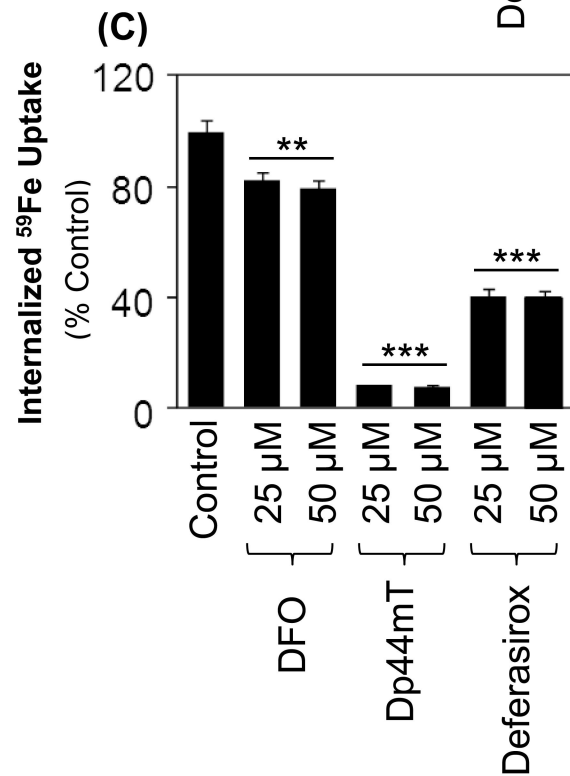
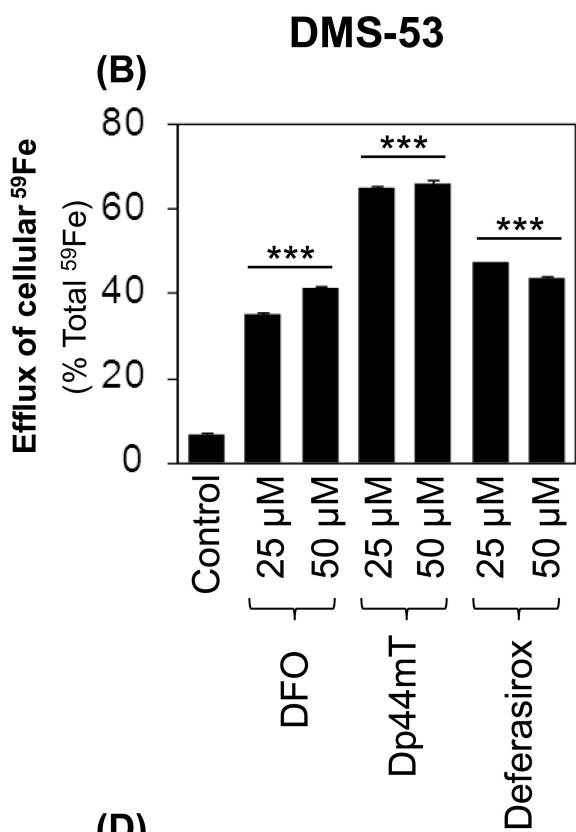
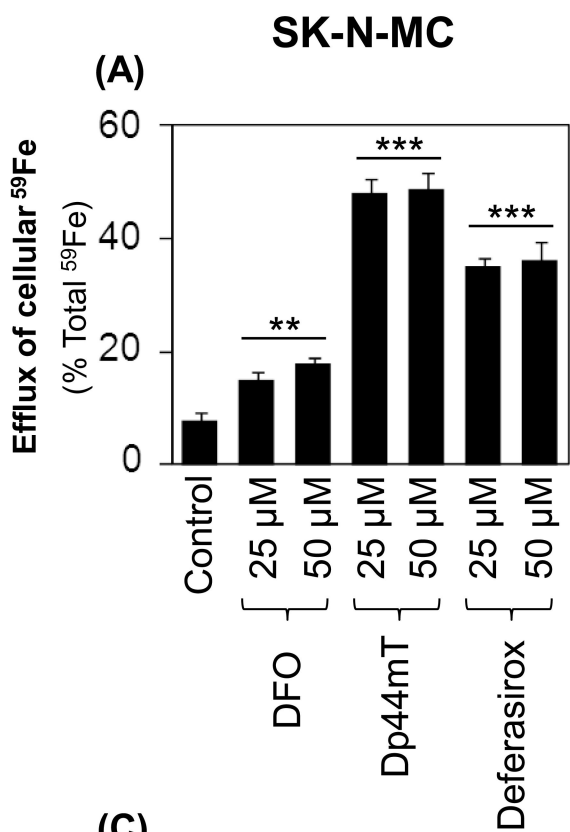
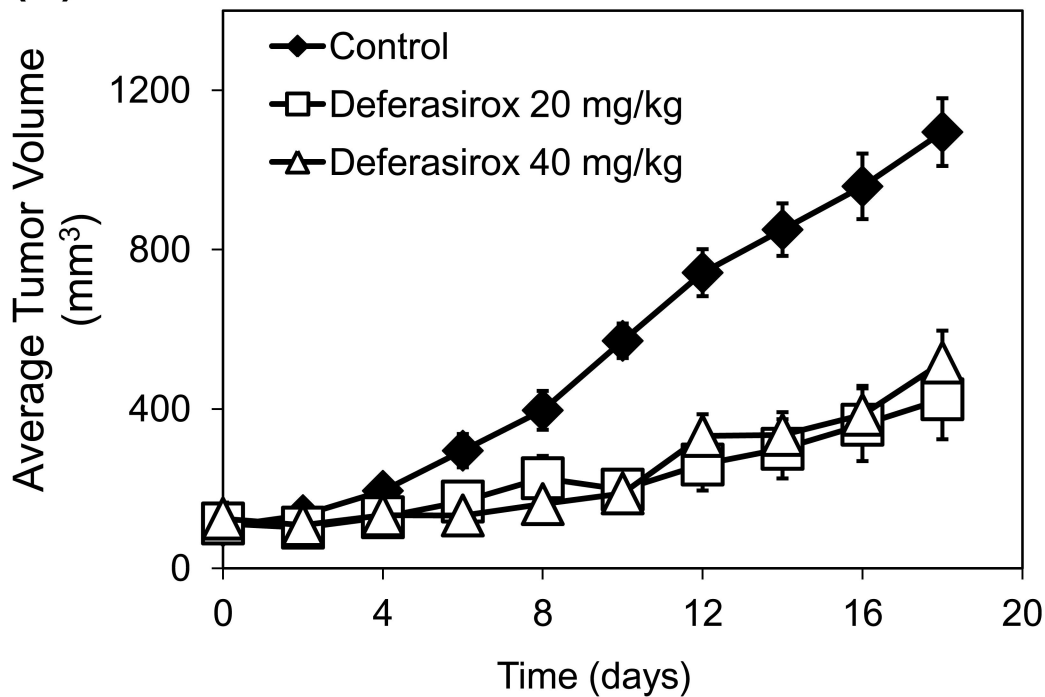
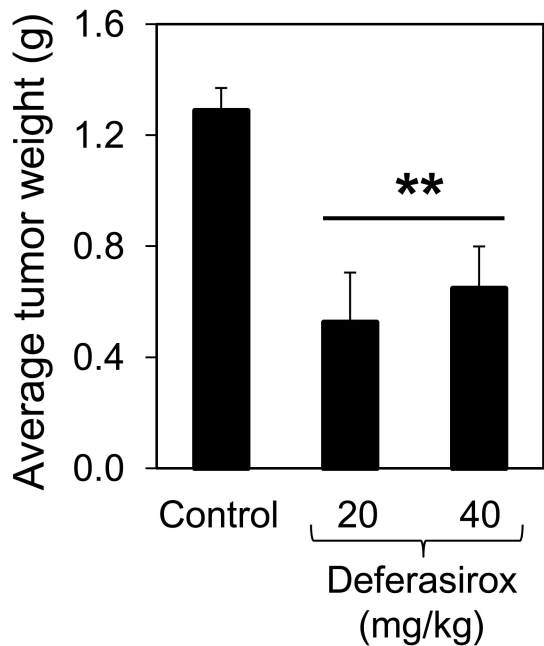
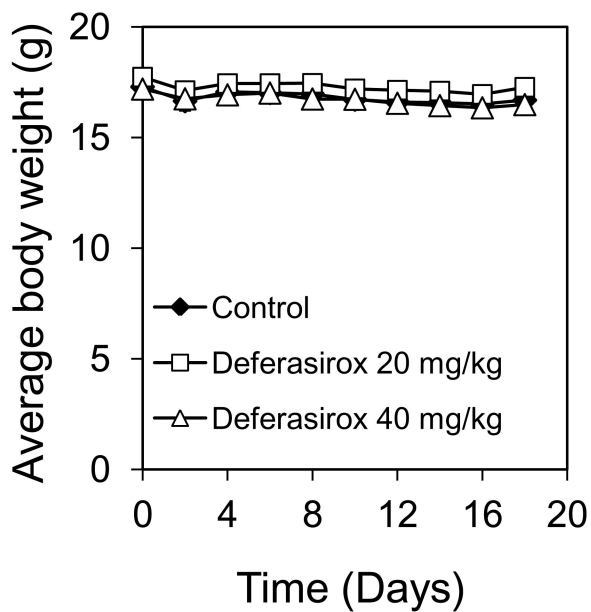


Figure 3

(A)**(B)****(C)****Figure 4**

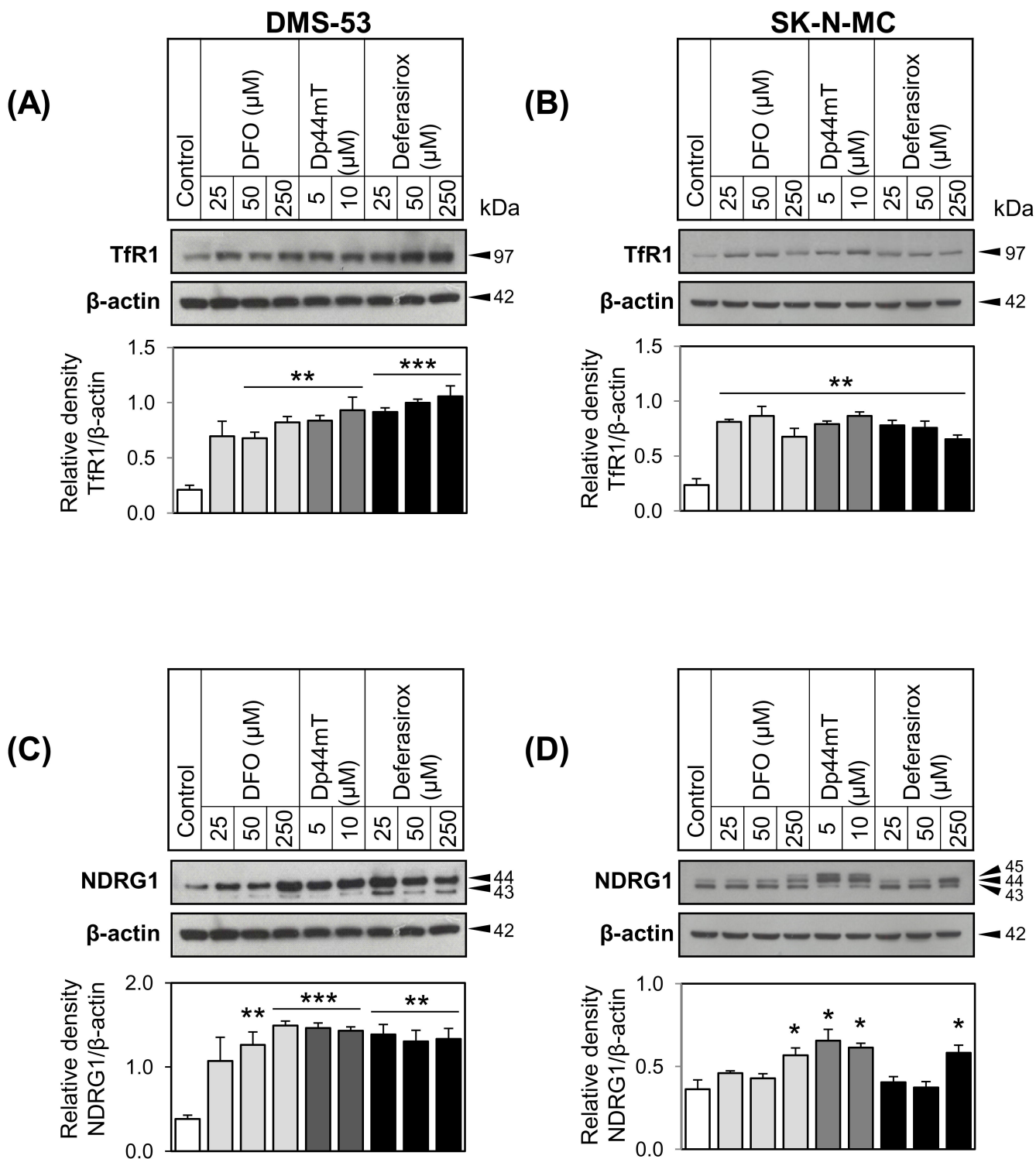


Figure 5

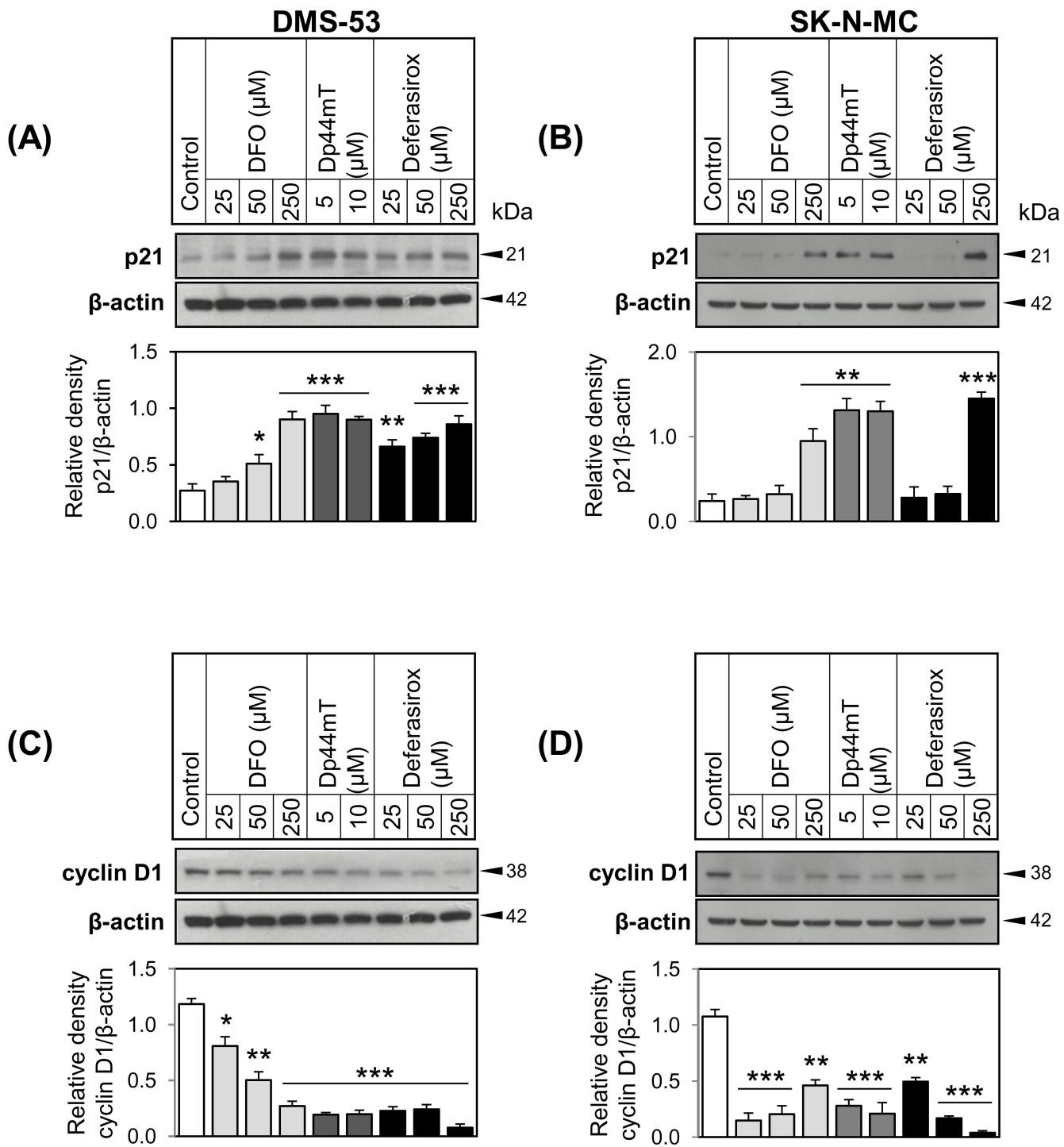


Figure 6

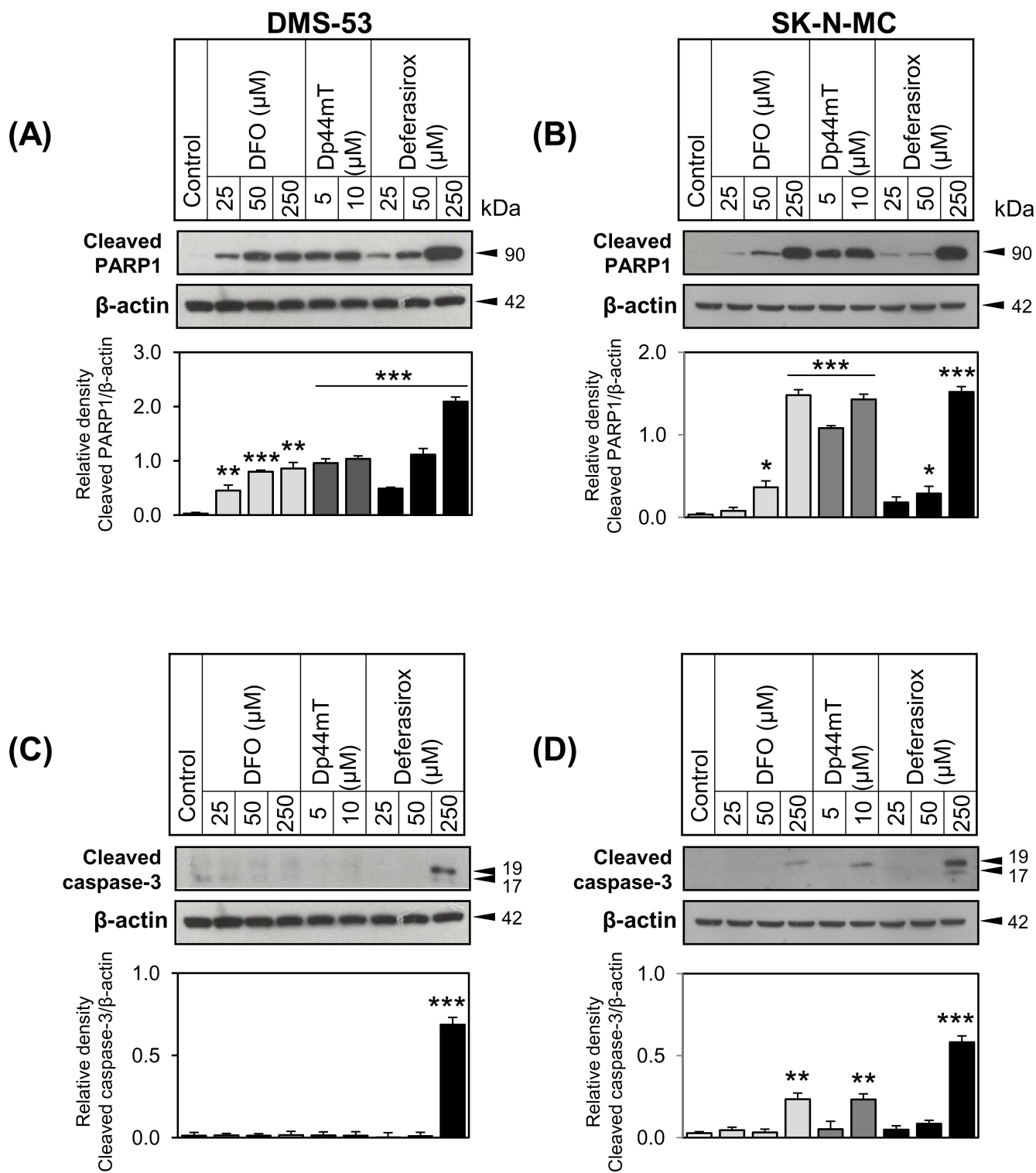


Figure 7

**The Iron Chelator, Deferasirox, as a Novel Strategy for Cancer Treatment:
Oral Activity Against Human Lung Tumor Xenografts and
Molecular Mechanism of Action**

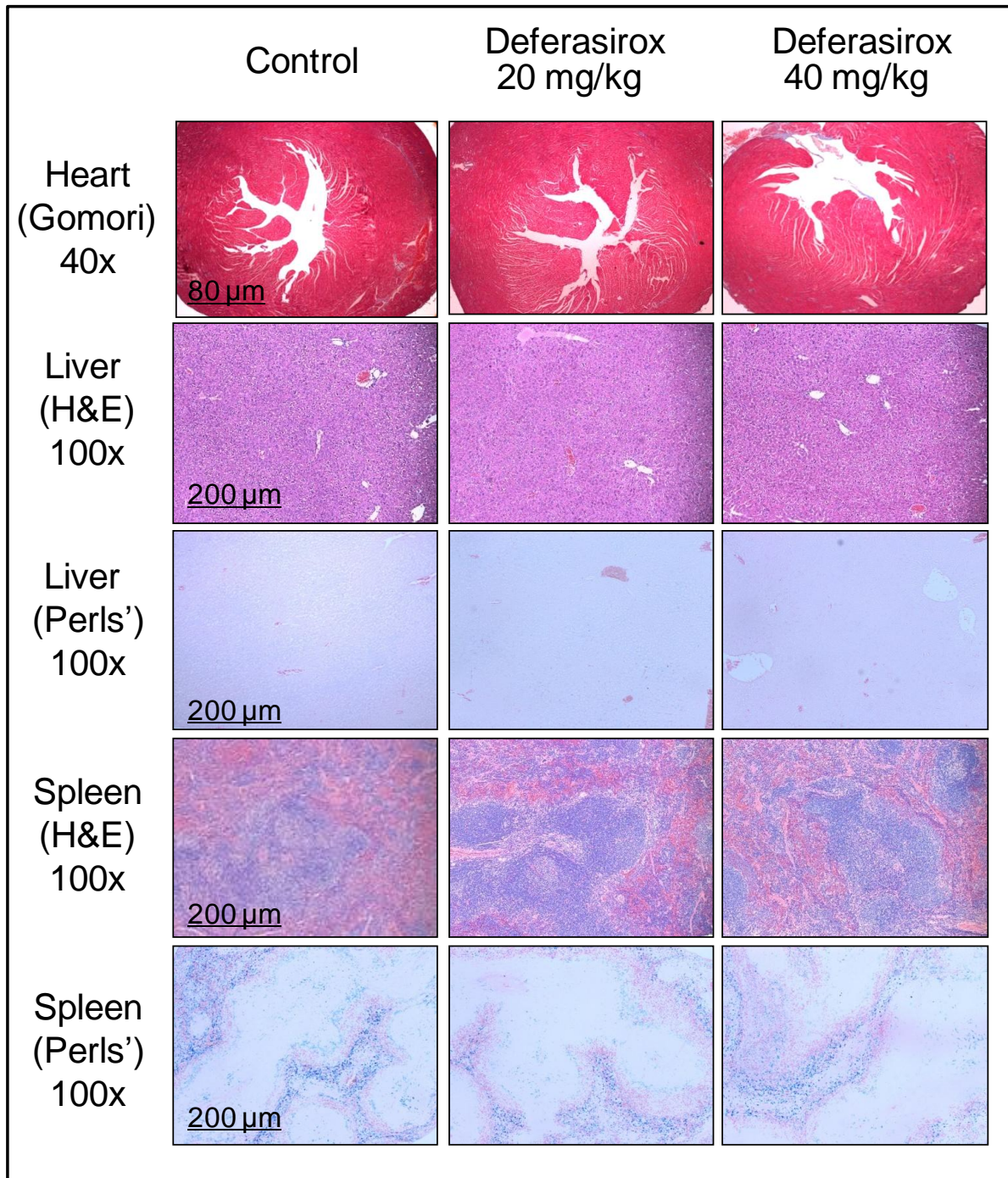
Goldie Y.L. Lui, Peyman Obeidy, Samuel J. Ford, Chris Tselepis, Danae M.
Sharp, Patric J. Jansson, Danuta S. Kalinowski, Zaklina Kovacevic, David B.
Lovejoy and Des R. Richardson

Molecular Pharmacology

Supplemental Data

Supplementary Table 1: Total tissue Fe, Cu and Zn levels in the liver, kidney and tumor from nude mice bearing a DMS-53 xenograft and treated orally by gavage with either the vehicle control or deferasirox (20 and 40 mg/kg; every 2nd day, 3 treatments per week) for 18 days. Values are expressed as mean \pm SEM. Statistical analysis was performed using the Student's *t*-test ($n=6$ mice/group); respective to vehicle control, * $p<0.05$.

| | | Treatment Groups | | |
|-----------|---------------|------------------|---------------|--------------|
| | | Vehicle Control | Deferasirox | |
| | Unit | | 20 mg/kg | 40 mg/kg |
| | Liver | 632 \pm 12 | 544 \pm 47 | 558 \pm 72 |
| Fe | Kidney | 305 \pm 18 | 306 \pm 16 | 290 \pm 21 |
| | Tumor | 140 \pm 23 | 128 \pm 19 | 134 \pm 26 |
| | | | | |
| | Liver | 22 \pm 3 | 23 \pm 1 | 29 \pm 4 |
| Cu | Kidney | 31 \pm 4 | 48 \pm 5 * | 46 \pm 4 * |
| | Tumor | 13 \pm 2 | 14 \pm 2 | 24 \pm 5 * |
| | | | | |
| | Liver | 99 \pm 3 | 103 \pm 6 | 118 \pm 13 |
| Zn | Kidney | 96 \pm 5 | 111 \pm 5 | 106 \pm 5 |
| | Tumor | 110 \pm 6 | 72 \pm 10 * | 84 \pm 11 |
| | | | | |



Supplementary Figure 1: Histopathology of heart, liver and spleen after oral administration of deferasirox to nude mice bearing human DMS-53 lung tumor xenografts. Nude mice bearing DMS-53 xenografts were treated with deferasirox (20 or 40 mg/kg orally; given by gavage every second day, 3 treatments/week for 18 days). Scale bar represents 80 μm in the images of the heart with 40x magnification, and 200 μm in the images of the liver and spleen with 100x magnification. Histological assessment was performed as described in the *Materials and Methods*.